Soft Matter

PAPER

View Article Online
View Journal | View Issue

Cite this: *Soft Matter*, 2017, 13, 686

Electrostatic interactions at the microscale modulate dynamics and distribution of lipids in bilayers†

Agustín Mangiarotti and Natalia Wilke*

Received 24th August 2016,
Accepted 13th December 2016

DOI: 10.1039/c6sm01957a

www.rsc.org/softmatter

For decades, it has been assumed that electrostatic long-range (micron distances) repulsions in lipid bilayers are negligible due to screening from the aqueous milieu. This concept, mostly derived from theoretical calculations, is broadly accepted in the biophysical community. Here we present experimental evidence showing that domain–domain electrostatic repulsions in charged and also in neutral lipid bilayers regulate the diffusion, in-plane structuring and merging of lipid domains in the micron range. All the experiments were performed on both, lipid monolayers and bilayers, and the remarkable similarity in the results found in bilayers compared to monolayers led us to propose that inter-domain repulsions occur mainly within the plane of the membrane. Finally, our results indicate that electrostatic interactions between the species inserted in a cell membrane are not negligible, not only at nanometric but also at larger distances, suggesting another manner for regulating the membrane properties.

1. Introduction

Biological membranes are open and complex systems, and due to their dynamic composition, understanding the principles that rule lateral organization and the relation with its functioning constitutes a challenging task. However, with the revolutionary work of Mueller and co-workers creating the "black lipid membranes" and the discovery of liposomes by Bangham *et al.*, the study of the lipid bilayer properties has grown in an exponential rate, and many other areas have been developed from the application of these model membranes.[1–3] One of the most studied aspects of membranes is the formation of lipid domains as a result of lipid phase segregation. The importance of these heterogeneities resides in the fact that these kinds of structures in cell membranes have been associated with protein sorting,[4–6] membrane traffic,[7] ion-channel regulation,[8] and signaling[9,10] among other cellular functions.

The observation of separate phases in lipid membranes was first described in Langmuir monolayers at the air–water interface using fluorescent probes that have a higher affinity for one of the coexisting phases.[11] Under certain conditions, these films presented modulated phases with thermodynamic or metastable (kinetically trapped) stability. The forces that led to a specific pattern of the membrane have been studied by analysing the structured lattices formed by the domains, and today we are able to predict and even tune-up the membrane texture by changing different parameters, like lipid composition,[12–17] the composition of the aqueous solutions,[18,19] the rate of nucleation,[12,20–23] the presence of lineactants,[24,25] among others.

While in monolayers pattern formation and modulated mesoscopic phases have been explained as a product of the competition between line tension and long-range electrostatic interactions due to the dipolar repulsions between the phases,[26–29] in bilayers, many researchers claimed that these interactions are only important at the nanoscopic scale since the membrane is immersed in an aqueous environment, and ionic screening reduces the dipolar interaction length scale. In some of the works dealing with this issue, theoretical calculations have been developed[30–32] while in others, it has simply been assumed.[27,33–37] Notwithstanding, there is a lack of experimental evidence sustaining these statements. It has to be recalled that both monolayers and bilayers represent very interesting electrostatic systems, since they are quasi-bidimensional arrangements with a dielectric constant varying from about 2 (hydrocarbon chains) to 80 (bulk water) within a nanometer sized region. Therefore, the question of what is the role played by electrostatics in these systems is challenging,

Centro de Investigaciones en Química Biológica de Córdoba (CIQUIBIC, UNC-CONICET), Departamento de Química Biológica, Facultad de Ciencias Químicas, Universidad Nacional de Córdoba, Haya de la Torre y Medina Allende, Ciudad Universitaria, X5000HUA, Córdoba, Argentina.
E-mail: wilke@mail.fcq.unc.edu.ar; Fax: +54-351-5353855; Tel: +54-351-5353855

† Electronic supplementary information (ESI) available: Details about domain coupling in bilayer systems (S1). Changes in %Lo in monolayers and in bilayers (S2). Image segmentation (S3). Domain tracking and diffusion measurements (S4). Videos showing domain diffusion and structuration in neutral (S5) and charged bilayers (S6). S5: real time lapse: 103.22 s (time between frames: 1.03 s) real size: (114.7 × 114.7) μm S6: real time lapse: 79.83 s (time between frames: 0.53 s) real size: (114.7 × 114.7) μm. See DOI: 10.1039/c6sm01957a

and thus in this work we used a set of experimental approaches with the aim of evaluating domain–domain interactions in bilayers. For that purpose, we used free-standing planar lipid bilayers, a version of the Montal and Mueller films obtained from monolayers,[38,39] which are very suitable for the study of membrane organization and dynamics since they enable real-time multi-domain and multi-bilayer imaging by direct microscope observation. In addition, in order to compare the results obtained from bilayers, we have also used Langmuir monolayers as a reference model, since they are well-studied systems in which domain interactions have already been described.[26–29]

We have analysed the Brownian motion, the position fluctuations and the merging of domains in neutral and charged lipid films. The selected lipid compositions are canonical raft mixtures. Our findings were very conclusive and shed new light on intra-membrane interactions, expanding the understanding of the complex bilayer behaviour.

2. Experimental

2.1 Materials

Dioleoylphosphatidylcholine (DOPC), dipalmitoylphosphatidylserine (DPPS), cholesterol (Chol), palmitoylsphingomyelin (pSM), and the lipophilic fluorescent probe L-α-phosphatidylethanolamine-*N*-(lissamine rhodamine B sulfonyl) (ammonium salt) (egg-transphosphatidylated, chicken) were purchased from Avanti Polar Lipids (Alabaster, AL).

Lipid mixtures were prepared in Cl_3CH/CH_3OH 2 : 1 v/v to obtain a solution of 1 nmol μL^{-1} total concentration with all the solvents and chemicals used being of the highest commercial purity available. The lipid monolayers and bilayers were prepared and characterized on subphases of 0.145 M NaCl at (22 ± 1) °C with water obtained from a Milli-Q system (Millipore), 18 MΩ cm.

Transmission electron microscopy (TEM) grids used for assembling the free-standing planar bilayers were obtained from SPI Supplies (West Chester, USA).

2.2 Methods

2.2.1 Lipid film observation. Canonical lipid raft mixtures containing a saturated lipid, an unsaturated lipid and cholesterol were used to perform the experiments. The mixtures DOPC : pSM (1 : 1) + 25% Chol and DOPC : DPPS (1 : 2) + 20% Chol were selected for experiments with neutral and charged domains, respectively. Compositions presenting phase segregation were chosen with the aim of observing and tracking the domains of the micrometric size in both monolayers and bilayers. For that purpose 1 mol% of the fluorescent probe was added to the mixtures. Since the fluorescent probe concentration in the denser phase was lower, domains in the liquid-ordered phase (Lo) appeared darker in the micrographs. The Lo phase was enriched in pSM and Chol or DPPS and Chol in each mixture.[40–44]

Lipid monolayers were prepared and characterized using a Langmuir film balance (microthrough, Kibron, Helsinki, Finland) placed on the stage of an inverted fluorescence microscope (Axiovert 200, Carl Zeiss, Oberkochen, Germany) with a 20×, 40× or a 100× objective. Images were registered using a CCD video camera (IxonEM+ model DU-897, Andor Technology).

Free-standing planar lipid bilayers were formed *via* Langmuir–Blodgett transfer using gold-coated TEM grids of 3 mm-diameter with 200 hexagonal perforations of 100 μm each. The gold surface was modified with octadecylthiol in order to generate hydrophobic substrates, as previously descripted.[39,45] Before carrying out the deposition, the grids were pretreated with 1 μL of 4% v/v hexadecane in hexane. Once hexane evaporates, the remaining hexadecane provides the proper Plateau–Gibbs border (torus) for bilayer formation.[40,46,47] In this manner, a monolayer containing the desired mixture was compressed up to 28 mN m^{-1}, and then the surface pressure was kept constant during the film transfer. This surface pressure is high enough for achieving an efficient film transfer, and low enough to still have phase segregation, since the critical points of these mixtures at 22 °C were near 33 mN m^{-1}. The substrate was lowered down vertically through the lipid interface and was placed parallel to the glass at the bottom of the trough in order to observe the bilayers using an inverted microscope. The bilayers remained under the subphase and were stable for hours.

The experimental setup allowed the *in situ* visualization of the monolayer and the bilayer after deposition as is depicted in Fig. 1A. Representative images of the monolayers and of the bilayers are also shown. A micrograph of a neutral monolayer before the film transfer is shown in Fig. 1B. Immediately after its transfer, the bilayer fluorescence appeared homogenous (see Fig. 1C), but after 10–15 minutes, phase segregation was observed (Fig. 1D and E). This lag time is concordant with the time required for the spontaneous thinning process due to solvent migration from the middle of the bilayer to the support borders.[47,48] Some bilayers break up during the transfer or by water flux when the grid is accommodated for observation, as can be observed at the bottom right of Fig. 1C. Additionally, a neutral and a charged bilayer is shown in Fig. 1D and E respectively. The analysed regions corresponded always to the centre of the bilayer in order to avoid effects due to the proximity to the Plateau–Gibbs border (square in Fig. 1E).

It should be noted that the bilayer domains used for this study are always coupled through both hemilayers, and only in isolated cases domains appeared decoupled, as proposed for this range of domain sizes (see the ESI,† S1).[49] The inter-domain repulsion was varied by decreasing the distances between domains of similar areas, which was achieved by increasing the amount of total area occupied by the liquid ordered phase (%Lo) as detailed in the ESI† (S2).

This is the first time, to our knowledge, that this bilayer system formed on TEM grids is used to see and study systems presenting phase segregation. Note that one of the advantages of this experimental set-up is that after transfer, a bilayer is formed in mostly all holes of the grid, allowing the analysis of multiple bilayers obtained from a single experiment, and improving the data acquisition and statistics.

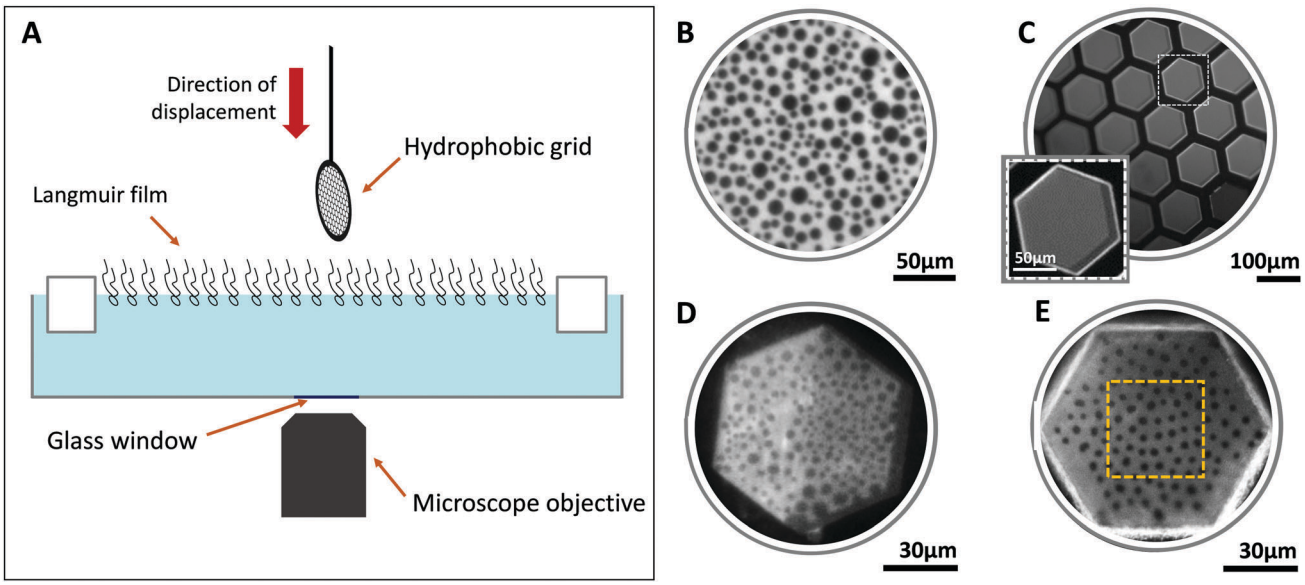

Fig. 1 Experimental setup used to generate and observe Langmuir monolayers and planar free-standing bilayers (A). Representative images showing a neutral Langmuir monolayer at a surface pressure of 28 mN m^{-1} (B), a grid immediately after transfer containing multiple homogeneous bilayers (C), and a magnification of the highlighted hole (inset in C), and a neutral (D) and a charged bilayer (E) showing the phase coexistence. The orange dashed square showed in (E) is an example of the region used for the analysis.

2.2.2 Domain tracking and diffusion measurements. In order to obtain diffusion coefficients (D) of domains, pairs of small domains (1–3 μm radius) were followed in videos of 15–20 seconds (150–200 frames, 0.1 s per frame) as described previously.[50] The software program Image-J was used to perform the image segmentation and the plugin "Mosaic Suite" allowed the tracking of particles through the images.[51] For more details and examples of image segmentation and trajectories obtained under convection drag, see the ESI† (S3 and S4).

2.2.3 Radial distribution function of domains and mean force interaction potentials. The radial distribution function $g(r)$ was calculated for domains at the membrane plane for bilayers and monolayers as a function of the amount of domains, quantified by the area percentage of the liquid ordered phase state, %Lo. Videos of 150 frames were divided into three parts, and histograms of the distance between domain centers (r) were constructed using data from 50 consecutive frames, and the reported $g(r)$ value was a result of averaging these histograms.

From the above determination, the mean force potential was calculated according to:

$$w(r) = -\beta^{-1} \ln g(r) \quad (1)$$

where β is $(kT)^{-1}$ and $w(r)$ represents the mean force potential between domains.[52] The first valley of the $w(r)$ curve (which corresponds to the first peak of the $g(r)$ curve) was fitted with a quadratic function and from its curvature an effective spring constant was calculated, which was used for quantifying the inter-domain interaction.

2.2.4 Domain merging. With the aim of quantifying the rate of fusion of the domains, videos of bilayers and monolayers were taken for 15–30 minutes with an interval of 5 seconds between frames. The amount of domains over time was calculated relative to the first micrography, and 12 photos were averaged for each minute. These videos were taken for membranes with 40%Lo for all systems, and at a fixed surface pressure of 28 mN m^{-1} in the case of Langmuir monolayers. Time zero was set at the moment of domain appearance in the case of bilayers, and at the point in which the desired surface pressure was reached for monolayers.

3. Results and discussion

3.1 Diffusion coefficient of liquid ordered domains

We measured the diffusion coefficient of small domains (D) in bilayers composed of DOPC : pSM (1 : 1) + 25% Chol (system with neutral domains) and DOPC : DPPS (1 : 2) + 20% Chol (system with charged domains) with the aim of analysing the effect that inter-domain interactions promote on the film dynamics. In Langmuir monolayers the determination of D has been used as an indirect way to gain insight into domain–domain repulsions. In this respect, it has been shown that hydrodynamic and electrostatic interactions (dipolar or Coulombic in the case of charged domains) preclude the movement of the domains as the inter-domain distances decrease leading to a higher apparent surface viscosity.[50,53] We used this well-known model system to compare the D values obtained with coupled domains in lipid bilayers at different percentages of area occupied by the liquid-ordered phase (%Lo), *i.e.* by the domains. For this purpose, the position of domains in different environments (different values of %Lo) was tracked. The obtained results are plotted in Fig. 2, where it can be observed that the values of the diffusion coefficient at low %Lo were lower for bilayers than for monolayers. This is because domains in bilayers were in contact with a viscous medium (water) both above and below, while the monolayers were formed at the air–water interface.

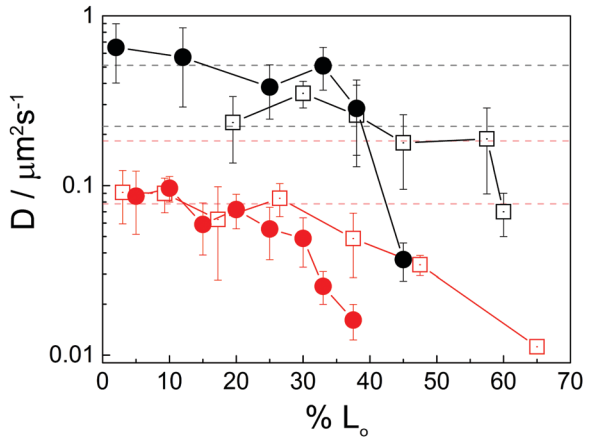

Fig. 2 Experimental values obtained for the diffusion coefficient (D) of small domains (1–3 μm) as a function of the percentage of area occupied by the liquid-ordered phase. Squares represent the neutral systems and circles the charged systems. The black colored symbols correspond to monolayers at the air–water interface and the red symbols to bilayers. The dashed lines correspond to the range of values of D_t calculated for the range of domain sizes, using eqn (2) or (3). The solid lines are drawn just to guide the eye.

The expected values of the diffusion coefficient (D_t) for isolated domains inserted in an expanded phase in the limiting case of $(R \times \eta_W)/\eta_m > 10$ can be calculated according to Hughes *et al.*[54] as follows:

$$D_t = (\beta 8 \eta_W R)^{-1} \quad \text{for monolayers} \qquad (2)$$

$$D_t = (\beta 16 \eta_W R)^{-1} \quad \text{for bilayers} \qquad (3)$$

where η_W = 0.001 N s m^{-2} is the water viscosity, η_m is the bidimensional membrane viscosity, and R is the radius of the domains under analysis. For bilayers, a factor of two is included in the denominator since water is present on both sides of the membrane.[54]

In Fig. 2, D_t values are plotted as a range delimited by dashed lines for lipid bilayers (red) and monolayers (black) taking into account the interval of the domain radius used for the analysis. In general, both membrane models showed a similar trend; when %Lo was low (high inter-domain distances) the inter-domain interactions were negligible and the experimental values matched the corresponding theoretical ones (eqn (2) and (3)) within errors.

The high values in monolayers (in the higher limit) may be related to an incomplete cancellation of the drift, while the low values in bilayers (in the lower limit) may be related to a higher viscosity of water close to the membrane surface. However, there is a fairly good match between the calculated and the experimentally determined diffusion coefficients for each system. This was expected, since when domains are distant from each other, they diffuse like isolated particles. The fact that the experimental D values at low %Lo fall into the range of the calculated values constituted a control and indicates that the method for tracking and quantifying the diffusion coefficients has yielded accurate values. On the other hand, for high %Lo, the experimental D values deviate from the predicted values as a result of repulsive forces between domains. Note that for charged domains (circles in Fig. 2) the diffusion coefficient decreased at lower values of %Lo and in a more pronounced fashion compared to neutral domains (squares), meaning that interactions were stronger in the presence of net charges.

It has been previously shown that the repulsive inter-domain interactions that affect domain diffusion in monolayers at micrometric distances are the dipolar or charge–charge interactions (for neutral and charged domains, respectively) and not hydrodynamic repulsions,[53] since a good correlation was found between the domain diffusion and the repulsive potential calculated from the equilibrium distribution of the domains. Furthermore, the distribution of domains in monolayers was found to strongly depend on the dipolar repulsive interactions.[55]

If inter-domain interactions in bilayers were negligible, the values of the diffusion coefficient of microscopic domains should fall within the values delimited by the red dashed lines in Fig. 2 even at 30–40%Lo. The decrease in the domain motion at high %Lo indicates the influence of inter-domain interactions at these percentages of the Lo phase, which could be related to electrostatic or hydrodynamic forces. In this regard, the remarkable similitude between domain diffusion in monolayers and bilayers points to a similar effect in both systems. Furthermore, the marked difference between the behaviour of charged *versus* neutral domains also points to electrostatic and not hydrodynamic repulsions, the last presumable being similar in both lipid mixtures.

At this stage, we anticipate that electrostatic inter-domain interactions in bilayers were not screened by the ionic solution as proposed previously,[30–32] the dipolar and charge–charge repulsive forces being not only appreciable at nanoscopic but also microscopic levels. These repulsions promoted a decrease of the values of the diffusion coefficient of microscopic domains at high values of %Lo.

In order to further prove the importance of electrostatic over hydrodynamic forces in lipid bilayers, the equilibrium domain distribution was analyzed, as presented in the following section.

3.2 Radial distribution function of domains in the plane of the membrane

In lipid monolayers at the air–water interface, there is a critical value of area occupied by domains (%Lo) in which dipolar repulsion leads to an ordered arrangement of the domains with fixed distances between them and even hexagonal arrays can be observed in the case of very structured lattices.[34,53,56,57] In this respect, the radial distribution function $g(r)$ provides an idea of the domain distribution in the plane of the membrane both in monolayers[53,55,56] and in bilayers.[34,36,37] At low %Lo values, the $g(r)$ function is expected to resemble that of a gas (without structure), while at higher percentage of the liquid ordered area, a peak corresponding to the nearest neighbour distance in an ordered array appears. If the distance value (r) at which the first peak appears exceeds the typical domain radius by a factor of about 3, the interaction that promotes domain ordering is expected to be different from mere hard-core repulsion between

the domains.[36] Additionally, as this is a distribution of positions and not a dynamic measurement, the hydrodynamic contributions do not influence the obtained results, and this approach gives account of repulsive interactions that affect the distances between domains and prevent them of being randomly distributed.[36,53]

We calculated $g(r)$ for the neutral and charged mixtures in both, bilayers and monolayers, at increasing percentages of the liquid-ordered area (area covered by domains). In this manner, the %Lo at which each film gained structure was determined. Interestingly, we found that monolayers and bilayers become structured at similar %Lo values: between 20–23% for neutral (Fig. 3A) and 16–19% for charged systems (Fig. 3B). Below those percentages no structure (peak in $g(r)$ function) was observed in the films and at higher %Lo the first peak became sharper (data not showed). Note that as a consequence of the difference in the size of the domains in each system, the peaks were shifted when comparing monolayers and bilayers. Domain area distribution is included for both model membranes as well as illustrative fluorescence images of the array of micro-domains.

The domains had sizes lying between 1–2 μm diameter and the distances between them (corresponding to the peaks of $g(r)$ function) in general for all systems were in the range of 4–7.5 μm.

The fact that domains acquired an ordered array at similar values of %Lo in bilayers compared to monolayers suggested that the inter-domain interactions that promote the ordering were similar in both systems. Furthermore, for charged systems the structuration took place at lower values of the liquid-ordered area in both monolayers and bilayers, indicating that the repulsion forces were stronger in the presence of a net charge, even with an ionic milieu (0.145 M NaCl). This fact further points to repulsions of the electrostatic origin. In our opinion, the non-negligible effect of electrostatic interactions on lipid bilayers at micrometric distances points to an important contribution of the repulsions within the plane of the membrane, leading to a similar influence of the forces in monolayers and in bilayers. In this sense, we have previously shown that the charge–charge interactions in monolayers can be reduced but not completely cancelled by decreasing the Debye–Hückel length to 0.55 nm, which is by far shorter than the analyzed inter-domain distances.[53]

3.3 Mean interaction force between domains in lipid bilayers

In order to get an estimation of the inter-domain electrostatic repulsions that promote domain structuring and preclude domain motion, we calculated the potential of mean force from the radial distribution functions obtained in the previous section, as explained in Section 2.2.3.[52] Fig. 4A shows an example for the calculation of the mean force potential between domains in the lattice of bilayers at 20%Lo in the case of neutral (squares) or charged (circles) domains. In this last case, a second valley (minimum) corresponding to the second proximal neighbour can be observed due to the high structuration of the film. Note that the curves have the shape of a pair potential interaction function (resembles a Lennard-Jones potential). Assuming a harmonic potential, a spring constant (k) for the mean force between domains was obtained by fitting the first valley of each curve to a quadratic function (see the inset in Fig. 4A). A comparison between the obtained values for

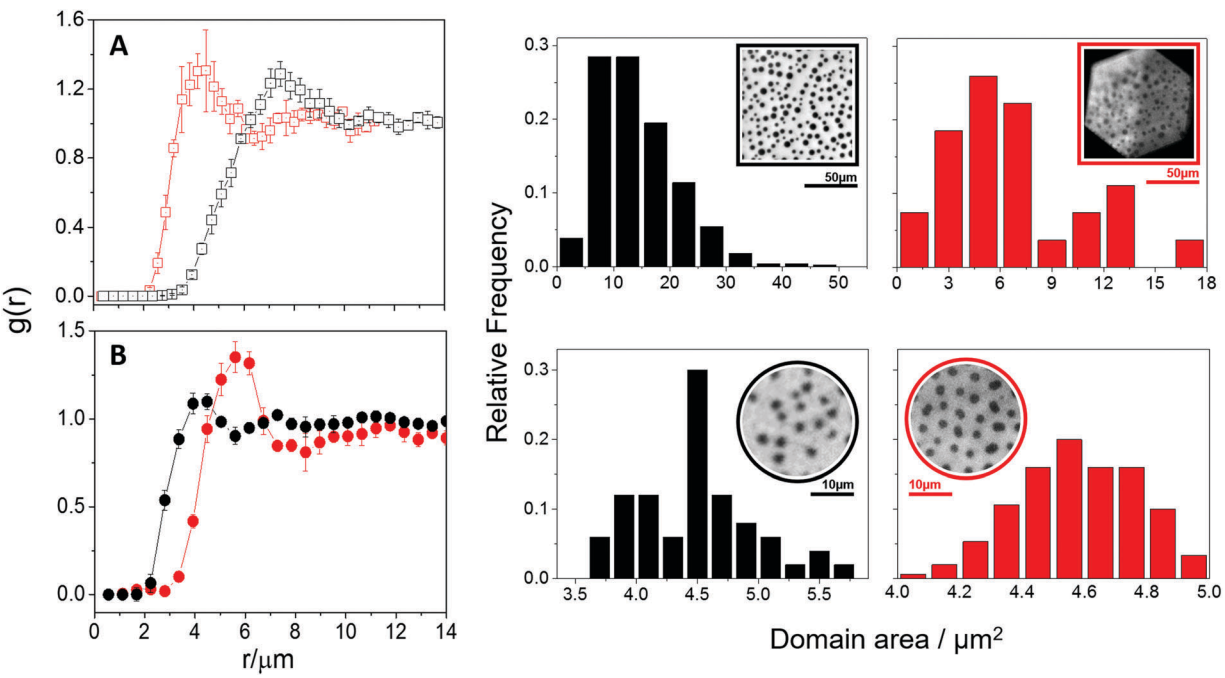

Fig. 3 Radial distribution functions for neutral (A) and charged (B) domains with their respective distribution of domain areas. Bilayers are shown in red and monolayers in black. The %Lo in (A) corresponds to 20–23%, and in (B) to 16–19% for monolayers and bilayers. Insets: Representative fluorescence images of the lipid films.

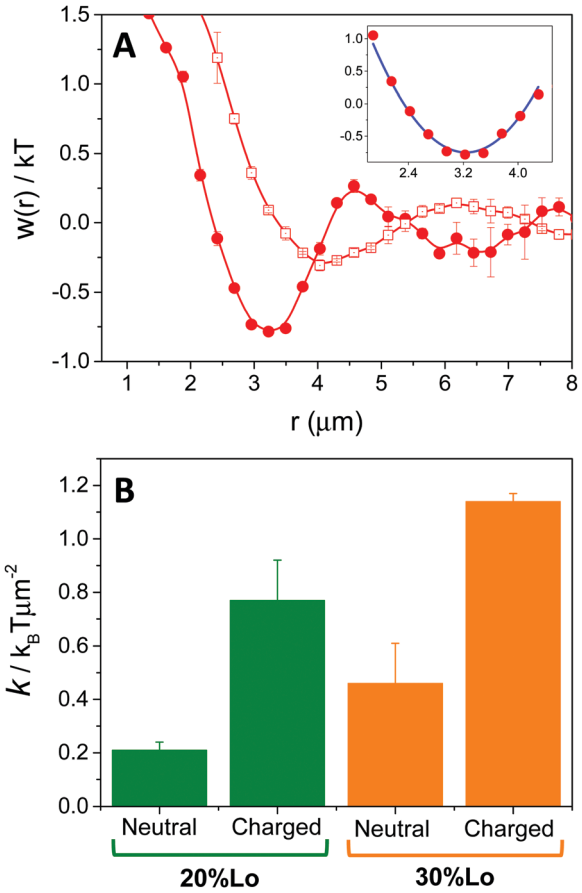

Fig. 4 (A) Mean force potential between domains $w(r)$ obtained from the analysis of images of bilayers with 20%Lo formed by charged (circles) or neutral (squares) domains. Inset: Example of the fitting to the experimental data (blue curve) corresponding to charged domains at 20%Lo. (B) Spring constant for a harmonic potential, obtained by fitting the first valley of $w(r)$ to a quadratic function (see the inset in A) for neutral and charged bilayers at the indicated liquid-ordered percentages.

k in neutral and charged bilayers at 20 and 30%Lo is shown in Fig. 4B. The interaction constant was 3–4 times higher for charged domains compared to neutral ones, and increased 1.5–2 times when changing from 20 to 30%Lo in both cases. This increase is expected since k was calculated using a mean field approach, thus being an effective interaction constant which increases as the amount of domains increases as a consequence of their approach. These results are in concordance with the diffusion measurements, when %Lo increased, the interaction between domains was higher (k increased), leading to a hindered domain motion.

The values of k found here were similar to those obtained in previous measurements of charged monolayers composed of DPPG under similar ionic conditions[53] and in neutral bilayers of DSPC and DMPC.[36] Those k values were calculated by tracking the position of a central domain in relation to the centre of mass of an array of 7 domains, assuming a Boltzmann distribution and local equilibrium. These similitudes indicate that the mean field potential of a domain in the array is mostly determined by the interaction of each domain with its closest neighbours.

3.4 Domain merging

In order to test the possible effects of the inter-domain repulsion in model membranes (aside from the membrane dynamics as shown in Section 3.1), the kinetic of domain merging was studied in each system.

The driving force for domain merging is line tension,[58] but the rate at which a domain approaches to its neighbour also commands the kinetics of merging. Due to Brownian motion, domains are able to collide and merge, however, as already shown in Section 3.1, domain motion is precluded at close inter-domain distances by the repulsions within each other. Therefore, domain merging depends on line tension, domain motion and inter-domain repulsions in a non-direct fashion,[59] and the rate of domain merge indirectly measures the repulsions between them. Hence, we monitored the amount of domains as a function of time for bilayers and monolayers of neutral and charged lipids with 40%Lo. Under these conditions, domains were initially close enough to each other as to allow them to fuse in short time-ranges. Fig. 5 shows a clear difference in the rate of merging of charged and neutral domains, and once more, the obtained values were similar for both, monolayers and bilayers. When domains were charged, no merge was observed in the analyzed window of time, thus the amount of domains remained constant. In contrast, when the membrane was formed by neutral molecules, the amount of domains decreased with time as a consequence of domain fusion, following the same trend for monolayers as for bilayers: in seven minutes the number of domains was reduced to 50% of the initial value. Semrau *et al.* observed in neutral vesicles the merging of domains, and they manage to prevent it by inducing curvature repulsions. They concluded that domains have to curve with respect to the other phase in order to give origin to repulsive interactions.[36] However, as already indicated, the rate of merging of domains depends on line tension, domain motion and inter-domain repulsion. All these factors depend in turn on the analyzed lipid mixture, and within a mixture, on the composition of the coexisting phases (*i.e.* the phase diagram of the mixture) and therefore the rate of merging changes from a system to other. In particular, for membranes close to a critical point, the difference in dipole density between phases becomes small.[60] This is the case of the studied systems, however neutral domains merged after tens of minutes and for charged domains, Coulombic repulsions prevented them from merging and led to a very organized lattice as can be observed in example videos (S5 and S6, ESI†) where the domains adopted almost fixed distances between them and the diffusion was slowed down in comparison to neutral films.

A rough estimation of the time that would take for two domains to touch each other can be performed taking into account the diffusion coefficient of isolated domains (0.1 $\mu m^2\ s^{-1}$, see Fig. 2). This value indicates that domains travelled in average 1 μm in about 1 s, and thus they should collide with other domains placed at 10 μm of distance (the average inter-domain distance at 40%Lo) in tens of seconds

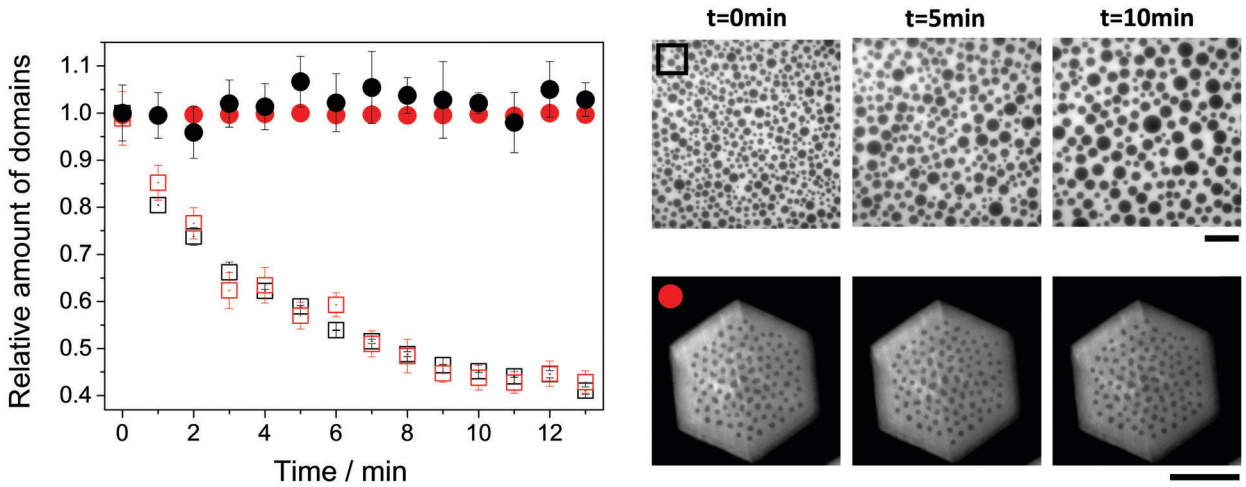

Fig. 5 Relative amount of domains *vs.* time for charged (circles) and neutral (squares) bilayers (red) or monolayers (black). The images are examples of a neutral monolayer (up) and a charged (down) bilayer at the indicated times. The symbol included in the images corresponds to the same symbol in the graphic. Scale bars correspond to 50 μm.

instead of tens of minutes as observed. Thus, the results shown in this section constitute another evidence of the importance of electrostatic interactions in lipid bilayers, showing that they have a measurable effect at the micron-scale and are strong enough to prevent or hinder the merging of domains for several minutes. The similarity between the rate of domain merging in monolayers and bilayers suggests similar inter-domain interactions. It has to be noted, however, that this comparison is far from being simple since the rate of domain motion is different (see Fig. 2) and line tension may also differ from a system to the other. In this regard, the estimated value for the line tension in the monolayers composed of DOPC : pSM (1 : 1) + 25% Chol was of the order of the pN whilst in bilayers, was an order of magnitude lower. This estimation was performed considering the rate at which two merged domains recovered the rounded shape. This difference in the line tension values was possibly caused by the shift in the phase diagram in monolayers compared to bilayers (see the ESI,† S2) as previously observed for other mixtures,[45] the bilayers being closer to the critical point thus showing a lower line tension value.

4. Summary and conclusions

In this study, we measured the effect of inter-domain interactions on the properties of planar lipid bilayers at the micron-scale using different approaches for neutral and charged domains. On the one hand, we determined dynamic parameters, such as diffusion of the domains and rate of domain merging. The first experiments showed that when the area occupied by the liquid-ordered phase was high, the domain movement was precluded due to the inter-domain repulsions, and a more marked effect was observed when domains were charged. With respect to domain merging, we have shown that domains fused at a slow rate for neutral membranes, and when they were charged, the strengthened interactions prevented them from merging in the measurement time-ranges. On the other hand, we performed static measures, allowing us to study the structuration of domains in the bilayer plane, and estimating a mean field interaction constant between them. We found that domains formed an ordered lattice at 22%Lo for neutral films and at 18%Lo for charged films on average. The mean field potential, which gives account of the interaction between domains, was stronger for charged domains compared to neutral ones, and their trend as %Lo increased correlated with the behaviour followed by the domain diffusion coefficients.

All the experiments performed in bilayers were also performed in monolayers of the same lipid composition and using solutions of the same ionic strength, and the results found for bilayers were remarkably similar to those in monolayers. This is an important result since in monolayers, electrostatic repulsions have been largely described and their influence is widely accepted by the scientific community.[14,26,28,29,53,55,61,62] Therefore, the similarity in the behaviour of domains in bilayers suggests non-negligible electrostatic interactions at micron ranges, and thus a not complete screening by the aqueous milieu. Furthermore, the inter-domain repulsions described here were present for coupled domains, indicating that the dipolar density in our system was not cancelled but prevailed, opposite to what was proposed to occur in symmetric domains reported by Travesset *et al.*[63] In turn, our results point out to an important contribution of in-plane inter-domain repulsions within the membrane. Inter-domain repulsions from non-electrostatic origins may also be present (*i.e.* curvature or height mismatch) but they are expected to be similar between the charged and the neutral systems. Therefore, the differences found between these systems are expected to be mostly due to electrostatic interactions.

In conclusion, far from being negligible, we showed that domain–domain electrostatic repulsions in bilayers appeared not only to be present but also to play a fundamental role in diffusive motion, interfacial structuring and merging of domains.

These forces, very probably occurring within the membrane plane, appear to be important at the micron-ranged length scale, and under physiological conditions. Therefore, electrostatic interactions between the species inserted in the cell membranes may account to a manner for regulating the membrane properties, and for communication of the molecules within the membrane. In addition to biological membranes, it is important to remark that these results may be relevant to other kinds of thin films with a mesoscopic structuration of dipolar or charged species.

Acknowledgements

This work was supported by SECyT-UNC, CONICET, and FONCYT (Program BID 0770), Argentina. N. W. is a career investigator and A. M. is a PhD fellow of CONICET. Authors wish to thank Dr Bruno Maggio for the revision and helpful discussion of the manuscript and José Ignacio Gallea for the table of content artwork design.

References

1 P. Mueller, D. O. Rudin, H. T. Tien and W. C. Wescott, *Circulation*, 1962, **26**, 1167–1171.
2 A. D. Bangham, B. A. Pethica and G. V. Seaman, *Biochem. J.*, 1958, **69**, 12–19.
3 Y.-H. M. Chan and S. G. Boxer, *Curr. Opin. Chem. Biol.*, 2007, **11**, 581–587.
4 D. Lingwood and K. Simons, *Science*, 2009, **327**, 46–50.
5 I. Mellman and W. J. Nelson, *Nat. Rev. Mol. Cell Biol.*, 2008, **9**, 833–845.
6 M. Stöckl, J. Nikolaus and A. Herrmann, in *Liposomes: Methods and Protocols, Biological Membrane Models*, ed. V. Weissig, Humana Press, Totowa, NJ, 2010, vol. 2, pp. 115–126.
7 M. F. Hanzal-Bayer and J. F. Hancock, *FEBS Lett.*, 2007, **581**, 2098–2104.
8 C. Dart, *J. Physiol.*, 2010, **588**, 3169–3178.
9 K. Simons and D. Toomre, *Nat. Rev. Mol. Cell Biol.*, 2000, **1**, 31–39.
10 A. F. G. Quest, J. L. Gutierrez-Pajares and V. A. Torres, *J. Cell. Mol. Med.*, 2008, **12**, 1130–1150.
11 H. M. McConnell, L. K. Tamm and R. M. Weis, *Proc. Natl. Acad. Sci. U. S. A.*, 1984, **81**, 3249–3253.
12 F. Vega Mercado, B. Maggio and N. Wilke, *Chem. Phys. Lipids*, 2012, **165**, 232–237.
13 M. Karttunen, M. P. Haataja, M. Saily, I. Vattulainen and J. M. Holopainen, *Langmuir*, 2009, **25**, 4595–4600.
14 S. Härtel, M. L. Fanani and B. Maggio, *Biophys. J.*, 2005, **88**, 287–304.
15 A. J. García-Sáez, S. Chiantia and P. Schwille, *J. Biol. Chem.*, 2007, **282**, 33537–33544.
16 F. A. Heberle, R. S. Petruzielo, J. Pan, P. Drazba, N. Kučerka, R. F. Standaert, G. W. Feigenson and J. Katsaras, *J. Am. Chem. Soc.*, 2013, **135**, 6853–6859.
17 J. M. Holopainen, H. L. Brockman, R. E. Brown and P. K. Kinnunen, *Biophys. J.*, 2001, **80**, 765–775.
18 F. V. Mercado, B. Maggio and N. Wilke, *Chem. Phys. Lipids*, 2011, **164**, 386–392.
19 A. Aroti, E. Leontidis, E. Maltseva and G. Brezesinski, *J. Phys. Chem. B*, 2004, **108**, 15238–15245.
20 M. L. Longo and C. D. Blanchette, *Biochim. Biophys. Acta, Biomembr.*, 2010, **1798**, 1357–1367.
21 A. E. McKiernan, T. V Ratto and M. L. Longo, *Biophys. J.*, 2000, **79**, 2605–2615.
22 U. Bernchou, J. Brewer, H. S. Midtiby, J. H. Ipsen, L. A. Bagatolli and A. C. Simonsen, *J. Am. Chem. Soc.*, 2009, **131**, 14130–14131.
23 M. L. Fanani, L. De Tullio, S. Hartel, J. Jara and B. Maggio, *Biophys. J.*, 2009, **96**, 67–76.
24 A. A. Bischof, A. Mangiarotti and N. Wilke, *Soft Matter*, 2015, 2147–2156.
25 P. Krüger and M. Lösche, *Phys. Rev. E: Stat. Phys., Plasmas, Fluids, Relat. Interdiscip. Top.*, 2000, **62**, 7031–7043.
26 H. McConnell, *Annu. Rev. Phys. Chem.*, 1991, **42**, 171–195.
27 T. M. Fischer and M. Losche, *Lect. Notes Phys.*, 2004, **634**, 383–394.
28 M. Seul and D. Andelman, *Science*, 1995, **267**, 476–483.
29 D. Andelman, *MRS Proc.*, 1989, **177**, 337–344.
30 J. Liu, S. Qi, J. T. Groves and A. K. Chakraborty, *J. Phys. Chem. B*, 2005, **109**, 19960–19969.
31 T. M. Konyakhina, S. L. Goh, J. Amazon, F. A. Heberle, J. Wu and G. W. Feigenson, *Biophys. J.*, 2011, **101**, L8–L10.
32 J. J. Amazon, S. L. Goh and G. W. Feigenson, *Phys. Rev. E: Stat., Nonlinear, Soft Matter Phys.*, 2013, **87**, 1–10.
33 H. M. McConnell and A. Radhakrishnan, *Biochim. Biophys. Acta, Biomembr.*, 2003, **1610**, 159–173.
34 S. Rozovsky, Y. Kaizuka and J. T. Groves, *J. Am. Chem. Soc.*, 2005, **127**, 36–37.
35 J. T. Groves, *Annu. Rev. Phys. Chem.*, 2007, **58**, 697–717.
36 S. Semrau, T. Idema, T. Schmidt and C. Storm, *Biophys. J.*, 2009, **96**, 4906–4915.
37 T. S. Ursell, W. S. Klug and R. Phillips, *Proc. Natl. Acad. Sci. U. S. A.*, 2009, **106**, 13301–13306.
38 M. Montal and P. Mueller, *Proc. Natl. Acad. Sci. U. S. A.*, 1972, **69**, 3561–3566.
39 C. W. Harland, M. J. Bradley and R. Parthasarathy, *Proc. Natl. Acad. Sci. U. S. A.*, 2010, **107**, 19146–19150.
40 A. V. Samsonov, I. Mihalyov and F. S. Cohen, *Biophys. J.*, 2001, **81**, 1486–1500.
41 B. L. Stottrup, D. S. Stevens and S. L. Keller, *Biophys. J.*, 2005, **88**, 269–276.
42 S. L. Veatch and S. L. Keller, *Phys. Rev. Lett.*, 2002, **89**, 268101.
43 F. Tokumasu, A. J. Jin, G. W. Feigenson and J. a. Dvorak, *Ultramicroscopy*, 2003, **97**, 217–227.
44 G. W. Feigenson, *Biochim. Biophys. Acta, Biomembr.*, 2009, **1788**, 47–52.
45 A. Mangiarotti, B. Caruso and N. Wilke, *Biochim. Biophys. Acta, Biomembr.*, 2014, **1838**, 1823–1831.
46 S. H. White, D. C. Petersen, S. Simon and M. Yafuso, *Biophys. J.*, 1976, **16**, 481–489.
47 A. Beerlink, S. Thutupalli, M. Mell, M. Bartels, P. Cloetens, S. Herminghaus and T. Salditt, *Soft Matter*, 2012, **8**, 4595.

48 W. D. Niles, R. a Levis and F. S. Cohen, *Biophys. J.*, 1988, **53**, 327–335.
49 S. May, *Soft Matter*, 2009, **5**, 3148.
50 N. Wilke and B. Maggio, *J. Phys. Chem. B*, 2009, **113**, 12844–12851.
51 I. F. Sbalzarini and P. Koumoutsakos, *J. Struct. Biol.*, 2005, **151**, 182–195.
52 L. Belloni, *J. Phys.: Condens. Matter*, 2000, **12**, R549–R587.
53 B. Caruso, M. Villarreal, L. Reinaudi and N. Wilke, *J. Phys. Chem. B*, 2014, **118**, 519–529.
54 B. D. Hughes, B. A. Pailthorpe and L. R. White, *J. Fluid Mech.*, 1981, **110**, 349–372.
55 E. Rufeil-Fiori, N. Wilke and A. J. Banchio, *Soft Matter*, 2016, **12**, 4769–4777.
56 N. Wilke, F. Vega Mercado and B. Maggio, *Langmuir*, 2010, **26**, 11050–11059.
57 S. Härtel, M. L. Fanani and B. Maggio, *Biophys. J.*, 2005, **88**, 287–304.
58 V. A. J. Frolov, Y. A. Chizmadzhev, F. S. Cohen and J. Zimmerberg, *Biophys. J.*, 2006, **91**, 189–205.
59 P. I. Kuzmin, S. A. Akimov, Y. A. Chizmadzhev, J. Zimmerberg and F. S. Cohen, *Biophys. J.*, 2005, **88**, 1120–1133.
60 S. Keller and H. McConnell, *Phys. Rev. Lett.*, 1999, **82**, 1602–1605.
61 N. Wilke and B. Maggio, *Biophys. Rev.*, 2011, **3**, 185–192.
62 D. Andelman, F. Broçhard and J. Joanny, *J. Chem. Phys.*, 1987, **86**, 3673–3681.
63 A. Travesset, *J. Chem. Phys.*, 2006, **125**, 0–12.

